Solids Modeled by ab Initio Crystal Field Methods. 21. Study of the Structure and Vibrational Spectrum of *N,N′*-Dimethylurea in the Gas Phase and in Its *Cc* Crystal Phase

R. Keuleers and H. O. Desseyn*

University of Antwerp (RUCA), Department of Chemistry, Groenenborgerlaan 171, B-2020 Antwerpen, Belgium

B. Rousseau and C. Van Alsenoy

University of Antwerp (UIA), Department of Chemistry, Universiteitsplein 1, B-2610 Antwerpen, Belgium

Received: January 6, 2000; In Final Form: March 17, 2000

In this study, the geometrical structure and vibrational spectrum are studied for the *N,N′*-dimethylurea molecule [$CO(NHCH_3)_2$] (DMU) in the gas phase as well as in its *Cc* crystal phase. The vibrational spectrum of DMU was interpreted by measuring the solid state state infrared spectra of normal, partially and totally deuterated DMU at room temperature and at −196 °C, and the Raman spectra of the solid state at room temperature and at −120 °C, and of DMU−water and DMU−chloroform solutions. Using calculations at the RHF/6-31++G** level, the equilibrium geometry and harmonic force field for both the gas phase and the crystal phase are determined. The crystal phase is modeled using a 15 molecule cluster surrounded by 6048 point charges.

I. Introduction

It has been shown that some Pt−urea complexes have antitumor activity,[1] probably due to their square-planar structure (e.g., cisplatinum). Moreover, the NH_2 and CO groups should provide enough hydrogen bonding to produce conformational changes in nucleotides and DNA in addition to chemical bonding. Because other urea complexes might also have this antitumor activity, we started to characterize these urea complexes. Therefore it was important to know the urea ligand very well. Although urea is one of the simplest biological molecules and has consequently extensively been studied, a lot of contradictions and uncertainties still seemed to exist certainly concerning the vibrational spectrum.[2] A thorough study on the vibrational analysis was necessary and was performed successfully in our previous study.[2−5] Calculated structure and frequencies were in excellent agreement with the experiments. As substitutes on the urea molecule also influence the metal−ligand bond and consequently the complex−nucleotide interaction, we also started to characterize the *N,N′*-dimethylurea (DMU) complexes. Again it was important to know the ligand very well, and on the basis of our succes for the urea molecule[2−5] we solved the vibrational spectrum of DMU in an analogous manner. Therefore the solid state infrared spectra of normal, partially, and totally deuterated DMU molecules were measured at room temperature and at −196 °C, just as the Raman spectra of the solid state at room temperature and at −120 °C, and of DMU−water and DMU−chloroform solutions. Force field calculations on the gas phase and on the solid state of DMU were performed at the Hartree−Fock level with a 6-31++G** basis set. To our knowledge no theoretical calculations on the solid-state structure or on the force field of any phase of DMU have been published yet.

Just as for urea it will be shown that the molecular cluster approach allows an accurate description of molecular crystals even in the case of extensively hydrogen bonded systems such as urea and DMU.

II. Experimental Section

1. General. The normal DMU used was a pure commercial product, available at Acros (11691−0010). Deuterated DMU was prepared by dissolving DMU in D_2O. Partially deuterated DMU were prepared by dissolving DMU in the corresponding H_2O/D_2O mixtures. The solutions were evaporated to dryness in vacuo. This procedure was repeated three times.

The infrared spectra were recorded on a Bruker IFS 113v Fourier Transform spectrometer, using a liquid nitrogen cooled MCT detector with a resolution of 1 cm^{-1}. For each spectrum 100 scans were recorded and averaged. The low-temperature measurements were performed with a laboratory designed liquid nitrogen cooled cryostat, consisting of a copper sample holder with a small container which can be filled with liquid nitrogen. This is surrounded by a jacket with KBr windows and placed under vacuum. From the sample a pellet with a KBr matrix was made. Far-infrared spectra were recorded using a DTGS detector with a resolution of 4 cm^{-1}. For each spectrum 250 scans were recorded and averaged.

The Fourier Transform Raman spectra were recorded on a Bruker IFS 66v interferometer equipped with a FT Raman FRA106 module. The molecules were excited by the 1064 nm line of a Nd:YAG laser operating at 200 mW. For each spectrum, 1000 scans were recorded and averaged. The low-temperature Raman spectra were recorded on a SPEX 1403−0.85 m double-beam spectrometer. The molecules were excited by the Spectra Physics model 2000 Ar^+ laser. A MILLER−HARNEY cell was used to cool the sample. The spectra were recorded with a spectral slit width of 4 cm^{-1}. For each spectrum 3 scans were recorded and averaged.

2. Theoretical Model & Computational Procedure. In this study the *Cc* crystal phase of DMU[6] was modeled using the supermolecule approach (SM-model) in which the supermol-

* To whom correspondence should be addressed.

10.1021/jp000094z CCC: $19.00
Published on Web 06/03/2000

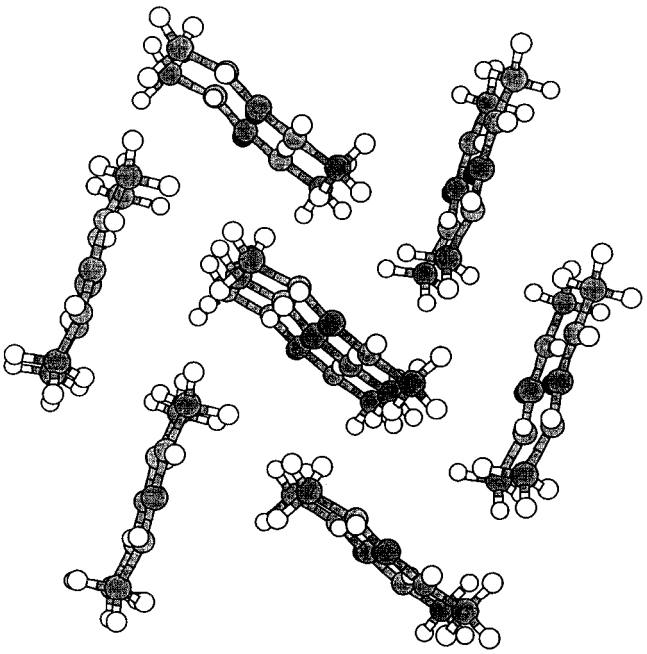

Figure 1. Projection of the 15 molecule cluster used to model the *Cc* crystal phase of DMU.

TABLE 1: Symmetry Operations Used to Generate the 14 nearest-Neighbors Surrounding a DMU Molecule

	symmetry operations		
0	x	y	z
1	$-^1/_2+x$	$-^1/_2-y$	$-^1/_2+z$
2	$-^1/_2+x$	$-^1/_2+y$	z
3	$-^1/_2+x$	$-^1/_2-y$	$^1/_2+z$
4	$x-1$	$-y$	$-^1/_2+z$
5	$x-1$	y	z
6	$-^1/_2+x$	$^1/_2+y$	z
7	$^1/+x$	$-^1/_2-y$	$-^1/_2+z$
8	$^1/_2+x$	$-^1/_2+y$	z
9	$^1/_2+x$	$-^1/_2-y$	$^1/_2+z$
10	x	$-y$	$-^1/_2+z$
11	$^1/_2+x$	$^1/_2+y$	z
12	x	$-y$	$^1/_2+z$
13	$x+1$	y	z
14	$x+1$	$-y$	$^1/_2+z$

ecule was constructed from a central molecule surrounded by its 14 nearest neighbors generated using the symmetry operations given in Table 1. For more details on this SM model, we refer to our previous articles.[2,3] A projection of the cluster is shown in Figure 1. This supermolecule was surrounded by molecules, represented by Mulliken pointcharges,[7] having an atom nearer to any central molecule atom than 20 Å, yielding 432 neighboring molecules (6048 point charges). A 6-31++G** basis set was chosen to describe the gasphase and the 15 molecule cluster. Use of this basisset resulted in a total of 162 basisfunctions describing the single molecule and 2430 basisfunctions describing the supermolecule used in this study.

A full geometry optimization was performed on DMU in both the gas phase and the solid state using standard gradient techniques[8] (fixing the unit cell parameters as well as the space group symmetry to their respective experimental values).[9] Optimized geometries were subsequently used in a numerical force field calculation for which analytic gradients were calculated at geometries described by displacements along the symmetry coordinates given in Table 2. Atom numbering is given in Figure 2. Frequencies for the isotopomer were calculated by solving the Wilson equation.[10]

III. Geometry of DMU in the Gas Phase, in DMU−water and DMU−chloroform Solutions, and in its *Cc* Crystal Phase

In the literature two publications have appeared describing the geometry of DMU, namely one theoretical calculation on the geometry in the gas phase[11] and one experimental structure determination on the solid state.[6]

From the Hartree−Fock calculation on the gas phase[11] using a 6-31G* basisset seemed that the hydrogen atoms, bound on the DMU nitrogens, are in a trans−trans position related to the C−O bond, and that the molecule is not planar around the nitrogen atoms with dihedral angles of 204.03° and 170.92° for the HNCO and (CH_3)NCN groups, respectively.

Figure 3 shows the crystal structure of DMU projected on the ac and the bc planes.[6] From this structure determination it seemed that in the solid state, the hydrogen atoms, bound on the DMU nitrogens, are in a trans−trans position related to the C−O bond as well. The non-hydrogen atoms are almost coplanar with the carbon atoms of the methyl group showing the largest deviation (0.035 Å) toward the plane of the NCON moiety. Both nitrogen atoms are connected in the a direction to the oxygen atom of a neighbor molecule through hydrogen bonds forming long parallel chains. The dipole moment within the different chains is always orientated in the a direction, as it is clearly visible on the projection on the ac plane, so that a polar structure is obtained.

Figure 4 shows the Raman spectra of DMU in the crystalline state, in a saturated $CHCl_3$ solution, and in a saturated and in a diluted H_2O solution. If we compare these spectra we clearly see that in solution four new bands at respectively 856, 648, 566, and 348 cm^{-1} appear and that the relative intensity of these bands increases from A to D. By comparing the profile and the relative intensity change of the band at 926 cm^{-1} in the solid-state spectrum, assigned to the ν_sC−N vibration, and the new band at 856 cm^{-1}, it can be stated that this new band can also be assigned to the ν_sC−N vibration. The extra bands at 648, 566, and 348 cm^{-1} are assigned to *N*-methyl bending vibrations. The fact that these new bands are superimposed on the spectrum observed for the solid state let us conclude that in these solutions DMU exists under two different conformations, namely, as dissolved clusters in which the different DMU interact (associate) in an analogous way as in the solid state, and as "isolated" molecules. This is also confirmed by the fact that in the $CHCl_3$ solution the new bands have a very low intensity indicating that the DMU molecules appear mainly in the conformation analogous to the solid state, or as dissolved clusters. In water, the DMU−DMU interactions are more and more replaced by DMU−solvent interactions when the relative amount of water to DMU increases explaining the higher relative intensity of the new bands assigned to the "isolated" DMU molecules. Because of the absence of DMU−DMU interactions it is, in analogy with urea,[2] no longer necessary that the conformation of the nitrogen atoms is (sp^2+p) as in the solid state. This is experimentally confirmed by the lower position of the ν_sC−N stretching vibration for the "isolated" DMU molecule and a new position of the N−CH_3 bending vibrations indicating a change in the N-conformation from (sp^2+p) to sp^3. Of course hydrogen bonds with solvent molecules still exist so that we can state, in analogy with urea,[2] that the dissolved state (sp^3, hydrogen bonds) can be seen as an intermediate state between the solid state (sp^2+p, hydrogen bonds) and the gas phase (sp^3, no hydrogen bonds), and consequently it is not correct to interpret the vibrational spectrum of solid DMU on the basis of a theoretical calculation on the gas phase.[2] Therefore, we started to perform

TABLE 2: Symmetry Coordinates of DMU (for Atom Numbers see Figure 2) Symmetry Assignments Are Those Based on a Planar C_2 Geometry)

	symmetry coordinates	assignment	S
1	$r(C_2-O_1)$	$\nu C-O$	A
2	$r(C_2-N_3) + r(C_2-N_5)$	$\nu_s C-N$	A
3	$r(C_2-N_3) - r(C_2-N_5)$	$\nu_{as} C-N$	B
4	$r(N_3-H_4) + r(N_5-H_6)$	$\nu_s N-H$	A
5	$r(N_3-H_4) - r(N_5-H_6)$	$\nu_{as} N-H$	B
6	$r(N_3-C_7) + r(N_5-C_8)$	$\nu_s N-R$	A
7	$r(N_3-C_7) - r(N_5-C_8)$	$\nu_{as} N-R$	B
8	$r(C_7-H_9) + r(C_7-H_{11}) + r(C_8-H_{12}) + r(C_8-H_{14})$	$\nu_s CH_3$	A
9	$r(C_7-H_9) + r(C_7-H_{11}) - r(C_8-H_{12}) - r(C_8-H_{14})$	$\nu_{as} CH_3$	B
10	$r(C_7-H_9) - r(C_7-H_{11}) + r(C_8-H_{12}) - r(C_8-H_{14})$	$\nu_s CH_3$	A
11	$r(C_7-H_9) - r(C_7-H_{11}) - r(C_8-H_{12}) + r(C_8-H_{14})$	$\nu_{as} CH_3$	B
12	$r(C_7-H_{10}) + r(C_8-H_{13})$	$\nu_s CH_3$	A
13	$r(C_7-H_{10}) - r(C_8-H_{13})$	$\nu_{as} CH_3$	B
14	$\theta(H_9-C_7-H_{10}) + \theta(H_9-C_7-H_{11}) + \theta(H_{10}-C_7-H_{11}) - \theta(H_9-C_7-N_3) - \theta(H_{10}-C_7-N_3) - \theta(H_{11}-C_7-N_3) + \theta(H_{12}-C_8-H_{13}) + \theta(H_{12}-C_8-H_{14}) + \theta(H_{13}-C_8-H_{14}) - \theta(H_{12}-C_8-N_5) - \theta(H_{13}-C_8-N_5) - \theta(H_{14}-C_8-N_5)$	$\delta_s CH_3$	A
15	$\theta(H_9-C_7-H_{10}) + \theta(H_9-C_7-H_{11}) + \theta(H_{10}-C_7-H_{11}) - \theta(H_9-C_7-N_3) - \theta(H_{10}-C_7-N_3) - \theta(H_{11}-C_7-N_3) - \theta(H_{12}-C_8-H_{13}) - \theta(H_{12}-C_8-H_{14}) - \theta(H_{13}-C_8-H_{14}) + \theta(H_{12}-C_8-N_5) + \theta(H_{13}-C_8-N_5) + \theta(H_{14}-C_8-N_5)$	$\delta_s CH_3$	B
16	$2\theta(H_9-C_7-H_{11}) - \theta(H_9-C_7-H_{10}) - \theta(H_{10}-C_7-H_{11}) + 2\theta(H_{12}-C_8-H_{14}) - \theta(H_{12}-C_8-H_{13}) - \theta(H_{13}-C_8-H_{14})$	$\delta_{as} CH_3$	A
17	$2\theta(H_9-C_7-H_{11}) - \theta(H_9-C_7-H_{10}) - \theta(H_{10}-C_7-H_{11}) - 2\theta(H_{12}-C_8-H_{14}) + \theta(H_{12}-C_8-H_{13}) + \theta(H_{13}-C_8-H_{14})$	$\delta_{as} CH_3$	B
18	$\theta(H_9-C_7-H_{10}) - \theta(H_{10}-C_7-H_{11}) + \theta(H_{12}-C_8-H_{13}) - \theta(H_{13}-C_8-H_{14})$	$\delta_s CH_3$	A
19	$\theta(H_9-C_7-H_{10}) - \theta(H_{10}-C_7-H_{11}) - \theta(H_{12}-C_8-H_{13}) + \theta(H_{13}-C_8-H_{14})$	$\delta_{as} CH_3$	B
20	$2\theta(H_{10}-C_7-N_3) - \theta(H_9-C_7-N_3) - \theta(H_{11}-C_7-N_3) + 2\theta(H_{13}-C_8-N_5) - \theta(H_{12}-C_8-N_5) - \theta(H_{14}-C_8-N_5)$	$\rho_s CH_3$	A
21	$2\theta(H_{10}-C_7-N_3) - \theta(H_9-C_7-N_3) - \theta(H_{11}-C_7-N_3) - 2\theta(H_{13}-C_8-N_5) + \theta(H_{12}-C_8-N_5) + \theta(H_{14}-C_8-N_5)$	$\rho_s CH_3$	B
22	$\theta(H_9-C_7-N_3) - \theta(H_{11}-C_7-N_3) + \theta(H_{12}-C_8-N_5) - \theta(H_{14}-C_8-N_5)$	$\rho_{as} CH_3$	A
23	$\theta(H_9-C_7-N_3) - \theta(H_{11}-C_7-N_3) - \theta(H_{12}-C_8-N_5) + \theta(H_{14}-C_8-N_5)$	$\rho_{as} CH_3$	B
24	$2\theta(N_3-C_2-N_5) - \theta(N_3-C_2-O_1) - \theta(N_5-C_2-O_1)$	δNCN	A
25	$\theta(N_3-C_2-O_1) - \theta(N_5-C_2-O_1)$	$\delta C-O$	B
26	$\omega(C_2,O_1,N_3,N_5)$	$\pi C-O$	B
27	$2\theta(C_2-N_3-C_7) - \theta(C_2-N_3-H_4) - \theta(C_7-N_3-H_4) + 2\theta(C_2-N_5-C_8) - \theta(C_2-N_5-H_6) - \theta(C_8-N_5-H_6)$	$\delta_s N-R$	A
28	$2\theta(C_2-N_3-C_7) - \theta(C_2-N_3-H_4) - \theta(C_7-N_3-H_4) - 2\theta(C_2-N_5-C_8) + \theta(C_2-N_5-H_6) + \theta(C_8-N_5-H_6)$	$\delta_{as} N-R$	B
29	$\theta(C_2-N_3-H_4) - \theta(C_7-N_3-H_4) + \theta(C_2-N_5-H_6) - \theta(C_8-N_5-H_6)$	$\delta_s N-H$	A
30	$\theta(C_2-N_3-H_4) - \theta(C_7-N_3-H_4) - \theta(C_2-N_5-H_6) + \theta(C_8-N_5-H_6)$	$\delta_{as} N-H$	B
31	$\omega(N_3,H_4,C_2,C_7) + \omega(N_5,H_6,C_2,C_8)$	$\pi_s N-H$	A
32	$\omega(N_3,H_4,C_2,C_7) - \omega(N_5,H_6,C_2,C_8)$	$\pi_{as} N-H$	B
33	$\tau(C_2-N_3-C_7-H_9) + \tau(H_4-N_3-C_7-H_9) + \tau(C_2-N_3-C_7-H_{10}) + \tau(H_4-N_3-C_7-H_{10}) + \tau(C_2-N_3-C_7-H_{11}) + \tau(H_4-N_3-C_7-H_{11}) + \tau(C_2-N_5-C_8-H_{12}) + \tau(H_6-N_5-C_8-H_{12}) + \tau(C_2-N_5-C_8-H_{13}) + \tau(H_6-N_5-C_8-H_{13}) + \tau(C_2-N_5-C_8-H_{14}) + \tau(H_6-N_5-C_8-H_{14})$	$\tau_{as} N-R$	B
34	$\tau(C_2-N_3-C_7-H_9) + \tau(H_4-N_3-C_7-H_9) + \tau(C_2-N_3-C_7-H_{10}) + \tau(H_4-N_3-C_7-H_{10}) + \tau(C_2-N_3-C_7-H_{11}) + \tau(H_4-N_3-C_7-H_{11}) - \tau(C_2-N_5-C_8-H_{12}) - \tau(H_6-N_5-C_8-H_{12}) - \tau(C_2-N_5-C_8-H_{13}) - \tau(H_6-N_5-C_8-H_{13}) - \tau(C_2-N_5-C_8-H_{14}) - \tau(H_6-N_5-C_8-H_{14})$	$\tau_s N-R$	A
35	$\tau(O_1-C_2-N_3-H_4) + \tau(N_5-C_2-N_3-H_4) + \tau(O_1-C_2-N_3-C_7) + \tau(N_5-C_2-N_3-C_7) + \tau(O_1-C_2-N_5-H_6) + \tau(N_3-C_2-N_5-H_6) + \tau(O_1-C_2-N_5-C_8) + \tau(N_3-C_2-N_5-C_8)$	$\tau_s C-N$	A
36	$\tau(O_1-C_2-N_3-H_4) + \tau(N_5-C_2-N_3-H_4) + \tau(O_1-C_2-N_3-C_7) + \tau(N_5-C_2-N_3-C_7) - \tau(O_1-C_2-N_5-H_6) - \tau(N_3-C_2-N_5-H_6) - \tau(O_1-C_2-N_5-C_8) - \tau(N_3-C_2-N_5-C_8)$	$\tau_{as} C-N$	B

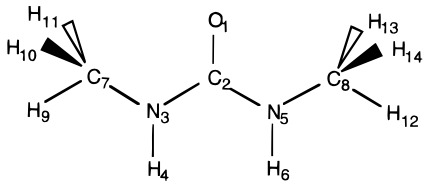

Figure 2. Atom numbering for the DMU molecule.

a theoretical calculation on the solid state of DMU in addition to the gas phase.

In Table 3 the calculated gas phase and the experimental and calculated solid-state geometries of DMU are compared.

A nonplanar geometry was calculated for the gas phase which is in full agreement with the Hartree−Fock calculation of Galabov.[11] For the solid state, a small deviation from planarity is also observed which is in full agreement with the results from the experimental structure determination.[6] The smaller deviation from planarity for the solid state compared to the gas phase is a consequence of the formation of a two-dimensional network of hydrogen bonds. In contrast to the experiment, the calculated structure is only slightly asymmetric as can be seen from the torsional angles given in Table 3. It should however be

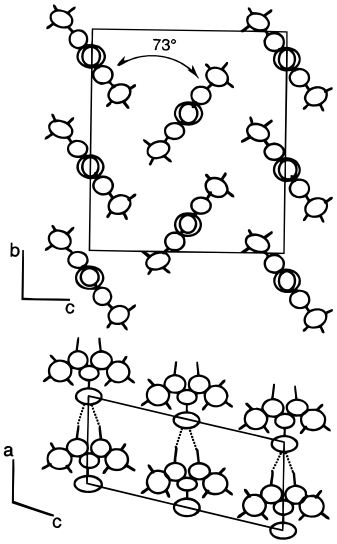

Figure 3. Structure of DMU in the crystalline state.

mentioned that given the large experimental uncertainties, a symmetric structure cannot be excluded. Taking into account

TABLE 3: Comparison Between Calculated and Experimental Structural Parameters for the Gas Phase and the Crystal Phase of DMU: Bond Lengths in angstroms, Bond Angles in Degrees[a]

	bond lengths					bond angles					torsional angles			
	gas phase	crystal phase				gas phase	crystal phase				gas phase	crystal phase		
	theor	theor	exptl	Δ		theor	theor	exptl	Δ		theor	theor	exptl	Δ
C2O1	1.204	1.209	1.242(5)	−0.033	N3C2O1	122.7	121.5	123.0(5)	−1.5	H4N3C2O1	158.0	168.3	−176.3	−15.4
C2N3	1.368	1.356	1.328(4)	0.028	N5C2N3	114.7	117.0	117.1(3)	−0.1	H6N5C2O1	158.0	167.6	−174.2	−18.3
C2N5	1.368	1.356	1.312(7)	0.044	C7N3C2	119.6	120.0	122.5(4)	−2.5	C7N3C2O1	9.51	12.0	3.0	9.0
N3C7	1.449	1.449	1.446(7)	0.003	C8N5C2	119.6	119.9	124.3(4)	−4.4	C8N5C2O1	9.53	11.9	6.5	5.4
N5C8	1.449	1.449	1.438(7)	0.011	H4N3C2	116.5	116.9			H4N3C2N5	−22.0	−11.7		
N3H4	0.998	0.995			H6N5C2	116.5	116.8			H9C7N3C2	−173.1	−175.9		
N5H6	0.998	0.995			H9C7N3	108.3	108.1			H10C7N3C2	−54.4	−57.6		
C7H9	1.087	1.086			H10C7N3	109.6	110.6			H11C7N3C2	66.2	64.1		
C7H10	1.084	1.082			H11C7N3	112.5	112.4			H12C8N5C2	−173.1	−175.7		
C7H11	1.090	1.088			H12C8N5	108.3	108.2			H13C8N5C2	−54.4	−57.5		
C8H12	1.087	1.086			H13C8N5	109.6	110.6			H14C8N5C2	66.2	64.2		
C8H13	1.084	1.082			H14C8N5	112.5	112.5							
C8H14	1.090	1.088												

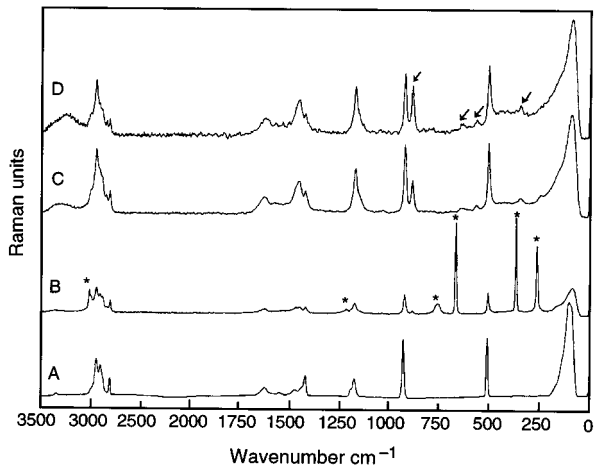

Figure 4. Raman spectra of DMU in the solid state (A), in a saturated $CHCl_3$-solution (B), in a saturated (C), and in a diluted (D) H_2O-solution.

TABLE 4: Fractional Atomic Coordinates and Equivalent Isotrophic Thermal Parameters (Å²)

	x	*y*	*z*	U_{eq}
O1	0.0194(7)	−0.1239(5)	−0.0002(6)	0.153(1)
C2	0.2916(7)	−0.1224(6)	0.0007(6)	0.129(1)
N3	0.4765(7)	−0.0434(4)	0.0652(5)	0.105(1)
H4	0.7080(7)	−0.0448(4)	0.0569(5)	0.118(1)
N5	0.4101(7)	−0.2061(4)	−0.0640(5)	0.113(1)
H6	0.6506(7)	−0.2069(4)	−0.0535(5)	0.123(1)
C7	0.3818(8)	0.0456(5)	0.1469(7)	0.120(1)
C8	0.2376(8)	−0.2947(5)	−0.1463(7)	0.136(1)

the level at which the calculations were performed, we can state from Table 3 that a good agreement between theory and experiment was obtained. Only for the HNCO torsional angles larger deviations were observed. However we would like to remark that these deviations are probably caused by some inaccuracies in the experimental X-ray structure determination. Table 4 gives the experimentally determined fractional atomic coordinates and the equivalent isotrophic thermal parameters.[6] Out of the thermal parameter of for example the oxygen atom we can determine the corresponding rms displacement as being 0.4 Å. For urea only 0.012 Å was experimentally observed.[12] Consequently, it can be stated that DMU vibrates more in its crystal lattice than urea so that it becomes nearly impossible to localize the electron of the hydrogen atoms, with a large error on the corresponding positions as a consequence.

Moreover from the 1014 measured reflections only 290 were observed above the noice. Consequently for every parameter varied only about four reflections were observed while for a standard experiment 10 to 40 reflections are found to be acceptable, pointing out again some inaccuracy in the experimental structure determination. Consequently we can consider our structure optimization as a further refinement of the experimental crystal structure. These optimized geometries were used in the further calculation of the force field and the "potential Energy distributions" (PEDs) of the corresponding vibrations.

TABLE 5: Definition of Groups of Symmetry Coordinates (See Table 2) Used in the Scaling of the Calculated Force Field with Optimized Scale Factors

crystal phase	gas phase
1:0.65	1:0.77
4,5:0.74	other:0.82
2,3,7,22,29,30,31:0.85	
other:0.81	

IV. The Vibrational Spectrum of DMU

The DMU molecule has fourteen atoms which leads to 42 degrees of freedom. Taking into account the six nongenuine motions (three translations + three rotations) 36 internal modes of vibration are to be considered. The symmetry of DMU is approximately C_2[6] giving rise to 18 A and 18 B modes. All the vibrational modes are infrared and Raman active. As for this molecule no splitting of the vibrational bands is observed (see further) it is not necessary, in contrast with urea,[4] to consider its factor group symmetry.

A. Force Field Calculation. Since it is well-known[13] that Hartree−Fock calculations overestimate the force constants, the calculated force constants are rescaled. Using a least-squares procedure four scale factors were optimized for the crystalline state. For this optimization all frequencies under 600 cm^{-1} were not considered (see further). As no experimental data were available for the gas phase of DMU the scale factors optimized for urea[3] were also used for DMU. The transferability of the scale factors will be shown to be acceptable further in this article based on our low-temperature measurements. Optimized values for these scale factors are given in Table 5.

These scale factors gave rise to a rms and largest deviation of 9 and 19 cm^{-1}, respectively, between the experimental and calculated frequencies of the solid state which is comparable to the results from our calculation on the urea molecule.[3] Terefore the frequencies under 600 cm^{-1} were again not considered (see further).

Calculated frequencies for the gas phase are given in Table 6. In Table 7 the experimental and calculated frequencies are compared for the crystal phase of DMU.

TABLE 6: Gas Phase Calculated Frequencies (cm^{-1}) and Potential Energy Distributions (PED) for the Parent and the Deuterated Isotopomer of DMU

DMU

	ν_{theor}	PED		ν_{theor}	PED
ν_sN−H (A)	3483	4 (100)	ν_sN−R (A)	1148	6 (41) − 2 (23) + 22 (21)
ν_{as}N−H (B)	3478	5 (100)	$\rho_{as}CH_3$ (B)	1139	23 (66) − 3 (11)
$\nu_s CH_3$ (A)	2994	12 (77) − 8 (15)	$\rho_s CH_3$ (B)	1123	21 (66) + 23 (13)
$\nu_{as} CH_3$ (B)	2994	13 (78) − 9 (15)	$\rho_s CH_3$ (A)	1120	20 (50) + 22 (29)
$\nu_{as} CH_3$ (B)	2951	11 (88)	ν_{as}N−R (B)	1004	7 (87)
$\nu_s CH_3$ (A)	2951	10 (88)	ν_sC−N (A)	902	2 (32) −20 (15) −24 (12) −27 (11) + 22 (11)
$\nu_s CH_3$ (A)	2884	8 (82) − 12 (10)	πC−O (B)	779	26 (90)
$\nu_{as} CH_3$ (B)	2883	9 (82) − 13 (11)	δC−O (B)	708	25 (42) − 28 (32)
νC−O (A)	1699	1 (68) − 2 (12)	δNCN (A)	496	2 (25) + 27 (21) + 6 (20) + 24 (14) − 31 (13)
δ_{as}N−H (B)	1550	30 (45) − 3(34)	π_{as}N−H (B)	453	32 (40) + 36 (27) − 3 (11)
δ_sN−H (A)	1495	29 (45) − 16 (13) − 18 (12)	π_sN−H (A)	367	31 (52) + 24 (18) + 35 (15)
$\delta_{as} CH_3$ (B)	1469	19 (56) + 17 (27)	δ_{as}N−R (B)	307	28 (46) + 25 (17) + 36 (15) + 32 (13)
$\delta_s CH_3$ (A)	1459	18 (56) + 29 (23)	δ_sN−R (A)	213	27 (54) − 24 (32)
$\delta_{as} CH_3$ (A)	1447	16 (62) + 14 (17)	τ_sC−N (A)	186	35 (54) − 31 (18) − 33 (17)
$\delta_{as} CH_3$ (B)	1447	17 (56) + 15 (18) − 19 (16)	τ_sN−R (A)	132	34 (83)
$\delta_s CH_3$ (B)	1428	15 (71) + 19 (17)	τ_{as}N−R (B)	117	33 (70) + 35 (18)
$\delta_s CH_3$ (A)	1423	14 (72) + 18 (13)	τ_{as}C−N (B)	112	36 (45) − 32 (42)
ν_{as}C−N (B)	1247	3 (33) + 30 (25) − 25 (16)			
$\rho_{as} CH_3$ (A)	1182	22 (30) − 6 (24) − 20 (20)			

DMU-d_2

	ν_{theor}	PED		ν_{theor}	PED
$\nu_s CH_3$ (A)	2994	12 (78) − 8 (15)	$\rho_{as} CH_3$ (B)	1129	23 (59) + 21 (31)
$\nu_{as} CH_3$ (B)	2994	13 (78) − 9 (15)	$\rho_s CH_3$ (A)	1129	22 (45) + 20 (42)
$\nu_{as} CH_3$ (B)	2951	11 (89)	ν_{as}N−R (B)	1015	7 (64) + 3 (16) + 30 (13)
$\nu_s CH_3$ (A)	2951	10 (88)	δ_sN−D (A)	960	29 (53) + 2 (20)
$\nu_s CH_3$ (A)	2884	8 (82) + 12 (10)	δ_{as}N−D (B)	915	30 (56) − 7 (21) − 26 (10)
$\nu_{as} CH_3$ (B)	2883	9 (82) + 13 (11)	ν_sC−N (A)	875	2 (25) + 6 (16) − 20 (15) − 29 (15)
ν_sN−D (A)	2554	4 (98)	πC−O (B)	765	26 (79) + 30 (10)
ν_{as}N−D (B)	2549	5 (99)	δC−O (B)	679	25 (48) − 28 (27) + 3 (12)
νC−O (A)	1688	1 (71) − 2 (14)	δNCN (A)	473	24 (25) + 2 (23) + 27 (22) + 6 (19)
ν_{as}C−N (B)	1478	3 (27) + 17 (27) + 19 (13)	π_{as}N−H (B)	367	32 (32) − 28 (27) + 36 (19) − 25 (12)
$\delta_s CH_3$ (A)	1472	18 (53) + 16 (31)	δ_{as}N−R (B)	294	32 (31) + 36 (28) + 28 (20)
$\delta_{as} CH_3$ (B)	1466	19 (46) − 15 (25) − 3 (13)	π_sN−H (A)	290	31 (63) + 24 (12)
$\delta_{as} CH_3$ (A)	1449	16 (52) − 18 (21) + 14 (19)	δ_sN−R (A)	210	27 (53) − 24 (34)
$\delta_{as} CH_3$ (B)	1441	17 (56) − 19 (23)	τ_sC−N (A)	175	35 (58) − 33 (27)
$\delta_s CH_3$ (A)	1423	14 (72) + 18 (14)	τ_sN−R (A)	131	34 (83)
$\delta_s CH_3$ (B)	1414	15 (60) − 3 (13) + 7 (12)	τ_{as}N−R (B)	116	33 (65) + 35 (24)
ν_sN−R (A)	1308	29 (31) + 6 (29) − 2 (23)	τ_{as}C−N (B)	112	36 (48) − 32 (41)
$\rho_s CH_3$ (B)	1177	21 (45) − 23 (26)			
$\rho_{as} CH_3$ (A)	1171	22 (33) − 6 (26) − 20 (19)			

From Table 7 we can state that, taking into account the level of the calculations, that a good agreement between theory and experiment has been obtained except for the low frequency region. These deviations are probably caused by a coupling of the corresponding vibrations with lattice vibrations. The latter, however, are not taken into account in our theoretical force field calculation. This coupling was not observed for urea.[2−4] However, urea has no absorptions in the low frequency area so that couplings between vibrations and lattice vibrations are energetically not favored. Moreover we have shown that DMU vibrates more in its lattice than urea which makes a coupling between vibrations and lattice vibrations more probable.

B. Vibrational Analysis of Crystalline DMU. The infrared spectrum of DMU has been described for the first time in 1954.[14] In this study Boivin tried to deduct the characteristic vibrational bands of the $CH_3NHCONH$ group by comparing a series of urea derivatives of the type $RNHCONHCH_3$ (R = alkyl, aryl). In 1956, Becher[15] deducted a coupling between the ν_{as}C−N and the δ_{as}N−H vibrations by comparing the infrared spectra of normal and deuterated DMU. In further studies a comparison was always made with the vibrational spectra of secundary amides of which it was known that the vibrational bands originated from coupled vibrations.[16] Furthermore, Yamaguchi[17] had also observed couplings in the vibrational spectrum of urea. This made several authors decide to perform a normal coordinate analysis so that the origin of the vibrational bands could be explained in function of potential energy distributions.[18−22] Experimentally the assignment of the vibrational spectrum has mainly been performed by comparing the infrared spectrum of normal and of deuterated DMU.[18,23−24] However, an experimental temperature study and a theoretical force field calculation on DMU have not been published yet.

The N−H and CH_3 Stretching Modes. In the infrared spectrum of DMU at room temperature the intense band at 3348 cm^{-1} with a weak shoulder at 3360 cm^{-1} disappear on deuteration and are consequently assigned to the N−H stretching vibrations. The corresponding N−D stretching vibrations are observed at respectively 2482 cm^{-1} with a weak shoulder at 2496 cm^{-1}. The average ratio νN−H/νN−D ≈ 1,35 indicates the pure character of these vibrations confirming the calculated PEDs in Table 7. The shift to lower frequency of these bands at lowering the temperature to −196 °C (3335 and 3357 cm^{-1}, respectively) is also indicative for N−H stretching character.[2] In the Raman spectrum only a weak broad band is observed at 3348 cm^{-1} which is shifted to lower frequency (3337 cm^{-1}) at lowering the temperature to −120 °C. After deuteration, this band is shifted to 2482 cm^{-1}, and a weak shoulder becomes visible at the high-frequency side of this band.

TABLE 7: Crystal Phase Experimental (−196 °C) and Calculated Frequencies (cm^{-1}) and Potential Energy Distributions (PED) for the Parent and the Deuterated Isotopomer of DMU

DMU

	ν_{theor}	ν_{exptl}	d	PED		ν_{theor}	ν_{exptl}	d	PED
ν_sN−H (A)	3352	3357	−5	4 (99)	ν_sN−R (A)	1162	1176	−14	6 (56) − 2 (21)
ν_{as}N−H (B)	3340	3335	5	5 (99)	ρ_{as}CH$_3$ (B)	1149	1165	−16	23 (55) − 21 (13)
ν_sCH$_3$ (A)	2999	2994	5	12 (69) − 13 (17) − 8 (11)	ρ_sCH$_3$ (A)	1131	1138	−7	20 (65) + 22 (15)
ν_{as}CH$_3$ (B)	2999	2994	5	13 (69) + 12 (17) − 9 (11)	ρ_sCH$_3$ (B)	1129	1117	12	21 (63) + 23 (25)
ν_sCH$_3$ (A)	2951	2947	4	10 (72) − 11 (26)	ν_{as}N−R (B)	1027	1042	−15	7 (87)
ν_{as}CH$_3$ (B)	2951	2947	4	11 (72) + 10 (26)	ν_sC−N (A)	914	933	−19	2 (27) − 20 (14) + 6 (13) + 22 (12) − 24 (12)
ν_sCH$_3$ (A)	2887	2904	−17	8 (86) + 12 (12)	πC−O (B)	782	776	6	26(92)
ν_{as}CH$_3$ (B)	2886	2883	3	9 (86) + 13 (12)	δC−O (B)	709	704	5	25 (45) − 28 (27)
νC−O (A)	1628	1621	7	1 (43) − 29 (30) + 24 (10)	τ_{as}C−N (B)	548	674	−126	36 (43) + 32 (35)
ν_{as}N−H (B)	1609	1595	14	30 (47) − 3 (36)	π_sN−H (A)	505			31 (22) − 27 (18) − 2 (18) + 35 (17) − 6 (12)
δ_sN−H (A)	1526	1542	−16	29 (39) − 2 (20) + 1 (17)	δNCN (A)	454	508	−54	35 (31) + 24 (28) + 31 (26)
δ_{as}CH$_3$ (B)	1476	1480	−4	19 (58) + 17 (17) − 15 (10)	δ_{as}N−R (B)	329	351	−22	28 (62) + 25 (24)
δ_sCH$_3$ (A)	1473	1477	−4	18 (57) − 14 (13)	δ_sN−R (A)	232	242	−10	27 (56) − 24 (33)
δ_{as}CH$_3$ (B)	1442	1453	−11	17 (58) + 15 (25)	τ_sC−N (A)	199			31 (49) − 35 (36)
δ_{as}CH$_3$ (A)	1441	1445	−4	16 (71)	τ_sN−R (A)	156			34 (69) + 33 (15)
δ_sCH$_3$ (B)	1427	1438	−11	15 (58) + 19 (23) − 17 (11)	τ_{as}N−R (B)	151	136	15	33 (63) − 34 (16)
δ_sCH$_3$ (A)	1419	1422	−3	14 (70) + 18 (15)	π_{as}N−H (B)	132			32 (70) − 36 (22)
δ_{as}C−N (B)	1281	1273	8	3 (39) + 30 (32) − 25 (13)					
ρ_{as}CH$_3$ (A)	1189	1195	−6	22 (58) − 6 (10)					

DMU-d_2

	$\nu_{theo.}$	ν_{exptl}	δ	PED		$\nu_{theo.}$	ν_{exptl}	δ	PED
ν_sCH$_3$ (A)	2998	2994	4	12 (64) − 13 (22)	ρ_{as}CH$_3$ (A)	1210	1220	−10	22 (63) − 6 (16)
ν_{as}CH$_3$ (B)	2998	2994	4	13 (64) + 12 (22)	ρ_sCH$_3$ (B)	1195	1194	1	21 (46) + 23 (38)
ν_sCH$_3$ (A)	2951	2951	0	10 (64) − 11 (33)	ρ_sCH$_3$ (A)	1189	1175	14	20 (58) + 6 (14)
ν_{as}CH$_3$ (B)	2951	2951	0	11 (64) + 10 (33)	ν_{as}N−R (B)	1024	1025	−1	7 (59) + 30 (19) + 3 (16)
ν_sCH$_3$ (A)	2886	2904	−18	8 (86) + 12 (12)	δ_sN−D (A)	984	984	0	29 (50) + 2 (20) 1 (12) − 6 (11)
ν_{as}CH$_3$ (B)	2885	2883	2	9 (86) + 13 (12)	δ_{as}N−D (B)	921	953	−32	30 (58) − 7 (28)
ν_sN−D (A)	2484	2483	1	4 (97)	ν_sC−N (A)	894	914	−20	2 (22) + 6 (20) − 29 (15) − 24 (11)
ν_{as}N−D (B)	2474	2475	1	5 (98)	πC−O (B)	773	770	3	26 (89)
νC−O (A)	1619	1619	0	1 (64) − 2 (16) + 24 (10)	δC−O (B)	688	643	45	25 (52) − 28 (27)
ν_{as}C−N (B)	1499	1521	−22	3 (41) + 17 (12)	δNCN (A)	473	498	−15	24 (30) + 27 (21) + 2 (21) + 6 (19)
δ_sCH$_3$ (A)	1488	1480	8	18 (54) + 16 (19) − 22 (11)	τ_{as}C−N (B)	426	423	3	36 (44) + 32 (36)
δ_{as}CH$_3$ (B)	1483	1477	6	19 (50) − 15 (16)	π_sN−D (A)	338			31 (42) + 35 (34)
δ_{as}CH$_3$ (A)	1450	1453	−3	16 (59) − 18 (17) + 20 (11)	δ_{as}N−R (B)	326	351	−25	28 (56) + 25 (21) + 36 (13)
δ_{as}CH$_3$ (B)	1444	1445	−1	17 (61) − 19 (19)	δ_sN−R (A)	229	242	−13	27 (53) − 24 (34)
δ_sCH$_3$ (A)	1421	1438	−17	14 (76) + 18 (11)	τ_sC−N (A)	194			31 (42) − 35 (41) + 33 (11)
δ_sCH$_3$ (B)	1417	1422	−5	15 (71)	τ_sN−R (A)	155			34 (69) + 33 (15)
ν_sN−R (A)	1323	1336	−13	29 (32) + 6 (22) − 2 (20)	τ_{as}N−R (B)	150	136	14	33 (61) − 34 (17)
ρ_{as}CH$_3$ (B)	1222	1231	−9	23 (42) − 21 (28)	π_{as}N−D (B)	132			32 (70) − 36 (22)

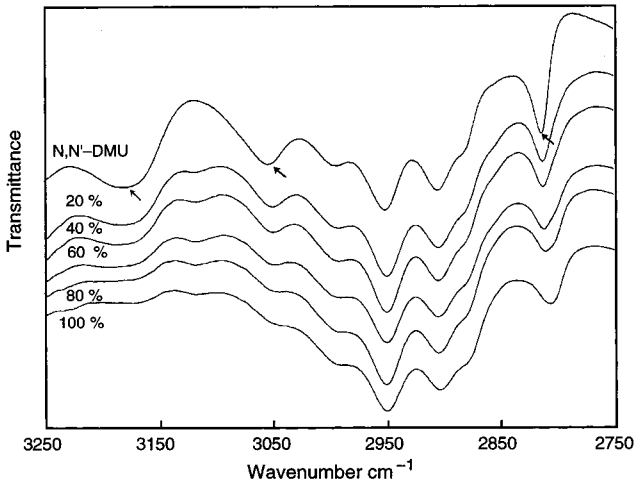

Figure 5. The 3250−2750 cm^{-1} region in the infrared spectra of partially deuterated DMU.

Figure 5 shows the 3250−2750 cm^{-1} region in the infrared spectra of partially deuterated DMU where the absorptions of the CH$_3$ stretching vibrations are expected. Very characteristic for this region is also the occurrence of overtones and combination bands of the νC−O, ν_{as}C−N, and δN−H vibrations.

In Figure 5 we clearly see that the bands at 3197, 3050, and 2813 cm^{-1} gradually decrease in intensity on deuteration so that they can be assigned to overtones or combination bands. The bands at 2994, 2947, 2904 cm^{-1}, and the shoulder at 2883 cm^{-1} stay invariant under deuteration and under lowering the temperature and can consequently be assigned to the CH$_3$ stretching vibrations. From our force field calculation on the solid state of DMU (Table 7), we learned that the νCH$_3$ bands occur each time two by two which makes that the two unobserved absorptions probably occur as weak shoulders on the bands at 2994 and 2947 cm^{-1}, respectively. In the Raman spectrum of DMU these vibrations are assigned to the shoulders at 2980 and 2885 cm^{-1}, and to the two intense bands at 2945 and 2904 cm^{-1}, which stay invariant under deuteration or under lowering the temperature.

The νC−O, νC−N, νN−R, and δN−H Vibrations of DMU. In the infrared spectrum of DMU, four bands at 1627 cm^{-1}, 1591, 1541, and 1270 cm^{-1} are observed because of the νC−O, ν_{as}C−N, δ_sN−H, and δ_{as}N−H vibrations repectively. Only the intense band at 1627 cm^{-1} shifts to lower wavenumber at lowering the temperature so that this band can be assigned to

TABLE 8: Crystal Phase Experimental (20 °C) and Calculated Frequencies (cm^{-1}) and Potential Energy Distributions (PED) for the νC−O, νC−N, νN−R, and δN−H Vibrations of DMU

	exptl	RHF/6-31++G**	PED
DMU	1627	1628	43% νC−O − 30% δ_sN−H + 10% δNCN
	1591	1609	47% δ_{as}N−H − 36% ν_{as}C−N
	1541	1526	39% δ_sN−H − 20% ν_sC−N + 17% νC−O
	1270	1281	39% ν_{as}C−N + 32% δ_{as}N−H + 13% δC−O
	1175	1162	56% ν_sN−R − 21% ν_sC−N
	1040	1027	87% ν_{as}N−R
	931	914	27% ν_sC−N + 14% $\rho_s CH_3$ + 13% ν_sN−R +12% $\rho'_s CH_3$ − 12% δNCN
DMU-d_2	1627	1619	64% νC−O − 16% ν_sC−N + 10% δNCN
	1517	1499	41% ν_{as}C−N + 12% $\delta_{as}CH_3$
	1336	1323	32% δ_sN−D + 22% ν_sN−R − 20% ν_sC−N
	1027	1024	59% ν_{as}N−R + 19% δ_{as}N−H + 16% ν_{as}C−N
	982	984	50% δ_sN−D + 20% ν_sC−N + 12% νC-O − 11% ν_sN−R
	950	921	58% δ_{as}N−D − 28% ν_{as}N−R
	917	894	22% ν_sC−N + 20% ν_sN-R − 15% δ_sN−D − 11% δNCN

the νC−O vibration. From our force field calculation on the solid state (Table 8),,it seems that this vibration is coupled with the δ_sN−H and the δNCN vibrations. In the Raman spectrum, the νC−O vibration is assigned to the medium intense, isolated band at 1626 cm^{-1} which shifts to 1613 cm^{-1} after deuteration, confirming the coupling of the νC−O and the δ_sN−H vibrations.

The intense infrared band at 1591 cm^{-1} shifts to higher wavenumber (1595 cm^{-1}) at lowering the temperature to −196 °C, and to lower wavenumber (1517 cm^{-1}) on deuteration, indicating a coupling between the ν_{as}C−N and δ_{as}N−H vibrations. The broad intense band at 1270 cm^{-1} and the medium intense band at 1541 cm^{-1} shift to higher wavenumbers (1273 and 1542 cm^{-1}, respectively) upon lowering the temperature to −196 °C, and disappear on deuteration; therefore, they can be assigned to the δ_{as}N−H and δ_sN−H vibrations, respectively. In the Raman spectra these vibrations are assigned to the weak bands at respectively 1590, 1280, and 1550 cm^{-1}. These assignments and the coupling of the ν_{as}C−N and the δ_{as}N−H vibrations are confirmed by our force field calculation on the solid state (Table 8).

From this table we also learn that in the normal DMU the ν_sC−N and the ν_sN−R vibrations are coupled, but that no coupling exists between the νC−N, νN−R, and δN−H vibrations. If we look however at the PED of the deuterated analogue we see that, just as in the case of the urea molecule,[2] a coupling of these vibrations with the δN−D vibrations has appeared after deuteration. This coupling is also confirmed by the experiments. In the infrared spectrum of normal DMU the ν_sN−R, ν_{as}N−R, and ν_sC−N vibrations can be assigned to the medium intense sharp bands at 1175, 1040, and 931 cm^{-1}, respectively. Only the band at 931 cm^{-1} shows a small shift to higher wavenumber (933 cm^{-1}) upon lowering the temperature to −196 °C, which is in full agreement with our assignment. We remark that the band at 1175 cm^{-1} largely coincides with a band originating from a ρCH_3 vibration. Figure 6 shows the infrared spectra of partially deuterated DMU in the 1200−900 cm^{-1} region.

We clearly see the bands at 1040 and 931 cm^{-1} disappear and four new bands appear at, respectively, 1027, 982, 950, and 917 cm^{-1}, on deuteration. These new bands have a broader profile and are shifted compared to the bands in the spectrum of the normal DMU, confirming the coupling of the νC−N, νN−R and δN−D vibrations, as it was also observed in the results from our force field calculation on the solid state (Table 8). The band at 1175 cm^{-1} exhibits a gradual shift to 1165 cm^{-1}. The latter however corresponds to a ρCH_3 vibration and coincided in the spectrum of normal DMU with the band corresponding to the ν_sN−R vibration, as it is already mentioned above.

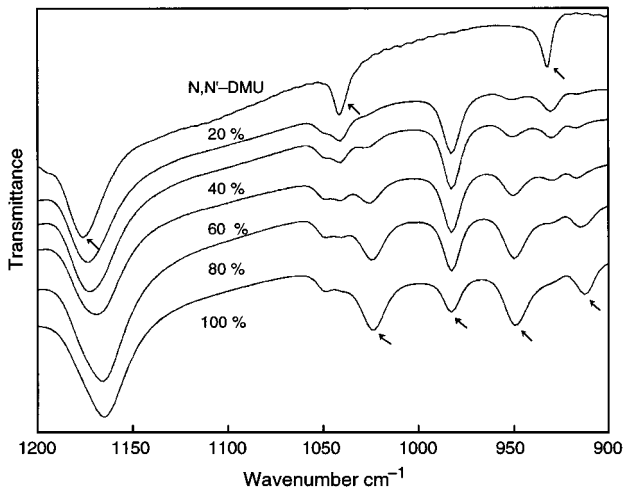

Figure 6. The 1200−900 cm^{-1} region in the infrared spectra of partially deuterated DMU.

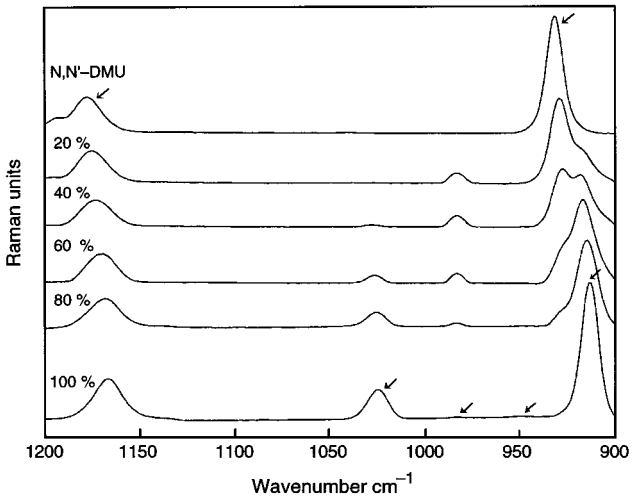

Figure 7. The 1200−900 cm^{-1} region in the Raman spectra of partially deuterated DMU.

Figure 7 shows the Raman spectra of partially deuterated DMU in the 1200−900 cm^{-1} region.

Just as in the infrared spectrum of DMU the band corresponding to the ν_sN−R vibration coincides with a band originating from a ρCH_3 vibration. The ν_{as}N−R band is too weak to be observed in the Raman spectrum. The ν_sC−N vibration is assigned to the very intense band at 931 cm^{-1} which shows a small shift to higher wavenumber (933 cm^{-1}) at lowering the temperature to −120 °C. After deuteration we see, just as in the infrared spectra, that the band at 1178 cm^{-1} is shifted to 1167 cm^{-1} and that in the 1050−900 cm^{-1} region four new bands have appeared, namely a medium intense band at 1025 cm^{-1}, two weak bands at 980 and 945 cm^{-1}, and an intense peak at 913 cm^{-1}, respectively. The very weak intensity of the bands at 980 and 945 cm^{-1} is very characteristic for high

δN−D character, which is in full agreement with our force field calculation on the solid state (Table 8). The shift of the intense band at 931 cm^{-1} to 913 cm^{-1} after deuteration is again indicative for a coupling between the νC−N, νN−R and δN−D vibrations, confirming again the results from our force field calculation on the solid state (Table 8).

For the assignment of the δCH_3 and the ρCH_3 vibrations we refer to Table 7. All these bands are, in the infrared and in the Raman spectrum, as expected, invariant under deuteration or under lowering of the temperature.

The δC−O and δCN and the "out-of-Plane" Vibrations of DMU. The mean intense, sharp infrared band at 775 cm^{-1} shows a small shift to higher a wavenumber (776 cm^{-1}) upon lowering the temperature to −196 °C, and is assigned to the πC−O vibration. In the Raman spectrum the πC−O peak is too weak to be observed. The very broad intense infrared band at 677 cm^{-1} disappears on deuteration. The profile of this band, its position in the vibrational spectrum and its attitude on deuteration, are characteristic for the π_{as}N−H vibration. In the Raman spectrum the corresponding peak is too weak and consequently not observed. On this band a shoulder is visible at 702 cm^{-1} which, upon lowering the temperature to −196 °C, shifts to a higher wavenumber (704 cm^{-1}). This shoulder, which is not observable in the Raman spectrum, is assigned to the δC−O vibration. The position of this band stays invariant under deuteration so that it can be stated that this vibration is not coupled with a N−H vibration, as it is also confirmed by our force field calculation on the solid state (Table 7). In the infrared and in the Raman spectrum of DMU a sharp intense band is also observed at 508 cm^{-1} of which the profile is characteristic for the δNCN vibration. In the far-infrared spectrum three strong absorptions are observed which stay invariant under deuteration. These bands are consequently assigned to the δ_{as}N−R, δ_sN−R, and τ_{as}N−R vibrations, respectively. The infrared and the Raman bands of the π_sN−H, π_{as}N−R, π_sN−R, and τ_sN−R vibrations are too weak to be observed.

As already mentioned, no splitting of the vibrational bands is observed, in contrast with urea,[2,4] so that it was not necessary to consider the factorgroup symmetry of DMU.

V. The Use of Low Temperature Measurements at the Vibrational Analysis of DMU, Transferability of the Scaling Factors for the Gas Phase of Urea To DMU

Table 9 shows the frequencies of all the infrared active vibrations of DMU at room temperature, at −196 °C and of our force field calculation on an isolated DMU molecule as a model for the gas phase. Therefore, we restricted ourselves to the region above 700 cm^{-1} because the PED's of the bands at lower frequencies differ too much between the gas phase and the crystal phase, due to the couplings of the corresponding vibrations with lattice vibrations in the crystalline state, and can consequently not be compared.[2]

If we look at the sequence of the DMU molecules in the gas phase, at room temperature and at −196 °C, we expect the molecules to come closer to each other, with stronger hydrogen bonds as a consequence.[2] Consequently, we expect to see the corresponding hydrogen bond dependent frequencies shift gradually on going from the gas phase to the solid state and further to −196 °C. If we look at Table 9, we see that the frequencies corresponding to the νCH_3, δCH_3, and ρCH_3 vibrations are practically identical for the gas phase, for the crystal phase at room temperature and for the solid state at −196 °C. This was to be expected as these vibrations are independent of the hydrogen bond strength between the different DMU molecules. Gradual shifts of the hydrogen bond dependent vibrations are also indeed observed in this table. The practically identical character of the CH_3 frequencies and the gradual shifts of the hydrogen bond dependent vibrational bands are indicative for the transferability of the scale factors of urea to DMU to obtain a good approximation for the gas phase spectrum. Only for the πC−O and the δC−O vibrations an opposite shift is observed when going from the room-temperature spectrum to the gas phase, and otherwise to the −196 °C spectrum, but the difference in frequency between the calculated value for the gas phase and the value for the room-temperature spectrum is so small that it can be considered as a consequence of a small deviation of the used scale factors. From this table we can also state for DMU, just as for urea,[2] that low-temperature measurements are very useful when performing a vibrational analysis as all the vibrational shifts can be very well explained in function of hydrogen bonding.

TABLE 9: Infrared Absorptions (cm^{-1}) of DMU in the Gas Phase and in the Crystal Phase at Room Temperature and at −196 °C

	gas phase (theor)		crystal phase 20 °C		crystal phase −196 °C
ν_sN−H (A)	3483	←	3360	←	3357
ν_{as}N−H (B)	3478	←	3348	←	3335
$\nu_s CH_3$ (A)	2994	=	2994	=	2994
$\nu_{as} CH_3$ (B)	2994	=	2994	=	2994
$\nu_{as} CH_3$ (A)	2951	←	2947	=	2947
$\nu_{as} CH_3$ (B)	2951	←	2947	=	2947
$\nu_s CH_3$ (A)	2884	→	2908	←	2904
$\nu_s CH_3$ (B)	2883	=	2883	=	2883
νC−O (A)	1699	←	1627	←	1621
δ_{as}N−H (B)	1550	→	1591	→	1595
δ_sN−H (A)	1495	→	1541	→	1542
$\delta_{as} CH_3$ (B)	1469	→	1480	=	1480
$\delta_s CH_3$ (A)	1459	→	1477	=	1477
$\delta_{as} CH_3$ (B)	1447	→	1453	=	1453
$\delta_{as} CH_3$ (A)	1447	←	1445	=	1445
$\delta_s CH_3$ (B)	1428	→	1438	=	1438
$\delta_s CH_3$ (A)	1423	←	1422	=	1422
ν_{as}C−N (B)	1247	→	1270	→	1273
$\rho_{as} CH_3$ (A)	1182	→	1195	=	1195
v_sN−R (A)	1148	→	1175	=	1176
$\rho_{as} CH_3$ (B)	1139	→	1165	=	1165
$\rho_s CH_3$ (A)	1123	→	1138	=	1138
$\rho_s CH_3$ (B)	1120	←	1117	=	1117
v_{as}N−R (B)	1004	→	1040	→	1042
ν_sC−N (A)	902	→	931	→	933
πC−O (B)	779	←	775	→	776
δC−O (B)	708	←	702	→	704

VI. Conclusions

This study on DMU in the *Cc* crystal phase shows, as in the case of the urea molecule,[3] that accurate geometries and frequencies can be obtained using the SM model, even in the case of extensively hydrogen bonded systems such as urea[3] and DMU.

In this study the geometry and the vibrational spectrum of DMU were solved by measuring the solid state infrared spectra of normal, partially and totally deuterated DMU at room temperature and at −196 °C, just as Raman spectra of the solid state at room temperature and at −120 °C, and of DMU−$CHCl_3$ and DMU−H_2O solutions. Geometry optimizations and force field calculations at the Hartree−Fock level with a 6-31++G** basis set, on an isolated DMU molecule and on the DMU molecule in its crystal structure were also performed. Therefore the crystal phase of DMU was modeled using a 15 molecule cluster surrounded by 6048 pointcharges.

In a last part of this article we have shown, as for urea,[2] that low-temperature measurements are very useful when performing a vibrational analysis as the observed spectroscopic shifts can very well be explained by the change of the hydrogen bond strength.

Acknowledgment. Robby Keuleers and Bart Rousseau thank the FWO and the IWT respectively for their grant. Christian Van Alsenoy thanks the FWO for an appointment as 'onderzoeksdirecteur' and the University of Antwerp for a grant GOA-BOF-UA nr. 23. The FWO is also acknowledged for the financial support for the spectroscopic equipment. The authors also thank Greta Thijs for the technical assistance and A.T.H. Lenstra for the discussion concerning the experimental structure determination.

References and Notes

(1) Theophanides, T.; Harvey, P. D. *Coord. Chem. Rev.* **1987**, *76*, 237.

(2) Keuleers, R.; Desseyn, H. O.; Rousseau, B.; Van Alsenoy, C. *J. Phys. Chem. A* **1999**, *103*, 4621.

(3) Rousseau, B.; Van Alsenoy, C.; Keuleers, R.; Desseyn, H. O. *J. Phys. Chem. A* **1998**, *102*, 6540.

(4) Rousseau, B.; Keuleers, R.; Desseyn, H. O.; Geise, H. J.; Van Alsenoy, C. *Chem. Phys. Lett.* **1999**, *302*, 55.

(5) Miao, M. S.; Van Doren, V. E.; Keuleers, R.; Desseyn, H. O.; Van Alsenoy, C.; Martins, J. L. *Chem. Phys. Lett.* Accepted for publication.

(6) Pérez-Folch, J.; Subirana, J. A.; Aymani, J. *J. Chem. Cryst.* **1997**, *27*, 367.

(7) Mulliken, R. S. *J. Chem. Phys.* **1955**, *23*, 1833.

(8) Pulay, P. *Mol. Phys.* **1969**, *17*, 197. Pulay, P. *Theor. Chim. Acta* **1979**, *50*, 299. Pulay, P. In *Ab initio Methods in Quantum Chemistry*; Lawley, K. P., Ed.; Advances in Chemical Physics LXIX; Wiley: New York, 1987; Part II, p 241.

(9) Swaminathan, S.; Craven, B. M.; McMullan, R. K. *Acta Crystallogr. B* **1984**, *40*, 300.

(10) Wilson, E. B., Jr.; Decius, J. C.; Cross, P. C. *Molecular Vibrations*; McGraw-Hill: New York, 1955.

(11) Galabov, B.; Ilieva, S.; Hadjieva, B.; Dudev, T. *J. Mol. Struct.* **1997**, *107*, 47.

(12) Vaughan, P.; Donohue, J. *Acta Crystallogr.* **1952**, *5*, 530.

(13) Pulay, P.; Fogarasi, G.; Boggs, J. E. *J. Chem. Phys.* **1981**, *74*, 3999. Fogarasi, G.; Pulay, P. Ab Initio Calculation of Force Fields and Vibrational Spectra. In *Vibrational Spectra and Structure*; Durig, J. R., Ed.; Elsevier Science: Amsterdam, 1985.

(14) Boivin, J. L.; Boivin, P. A. *Can. J. Chem.* **1954**, *32*, 561.

(15) Becher, H. J.; Griffel, F. *Die Naturwissenschaften* **1956**, *43*, 467.

(16) Rao, C. N. R. Chemical Applications of Infrared Spectroscopy; Academic Press: New York, 1963.

(17) Yamaguchi, A.; Miyazawa, T.; Shimanouchi, T.; Mizushima, S. *Spectrochim. Acta* **1957**, *10*, 170.

(18) Rao, C. N. R.; Chaturvedi, G. C.; Gosavi, R. K. *J. Mol. Spectrosc.* **1968**, *28*, 526.

(19) Mido, Y.; Murata, H. *Bull. Chem. Soc. Jpn.* **1969**, *42*, 3372.

(20) Ravindranath, K.; Balasubramanian, V.; Ramiah, K. V. *Indian J. Pure Appl. Phys.* **1976**, *14*, 58.

(21) Mido, Y.; Fujita, F.; Maztsuura, H.; Machida, K. *Spectrochim. Acta* **1981**, *A37*, 103.

(22) Geidel, E.; Böhlig, H.; Salzer, R.; Geiseler, G. *Monatshefte für Chemie* **1988**, *119*, 439.

(23) José, C. I. *Spectrochim. Acta* **1969**, *A25*, 111.

(24) Mido, Y. *Spectrochim. Acta* **1972**, *A28*, 1503.

(25) [a]Hydrogen bond distances and angles: theor (exptl;Δ). N3···O: 2.892 (2.86;0.03). H4···O: 2.008(1.88;0.13). N3H4···O: 146.9 (148.4;−1.5). H4···OC: 146.6(145.1;1.5). N5···O: 2.894 (2.87;0.02). H6···O: 2.006 (1.90;0.11). N4H6···O: 147.3 (147.7;−0.4). H6···OC: 146.8 (145.6;1.2).